Arch Toxicol (2016) 90:817–828
DOI 10.1007/s00204-015-1493-x

NANOTOXICOLOGY

Indium oxide (In_2O_3) nanoparticles induce progressive lung injury distinct from lung injuries by copper oxide (CuO) and nickel oxide (NiO) nanoparticles

Jiyoung Jeong · Jeongeun Kim · Seung Hyeok Seok · Wan-Seob Cho

Received: 27 August 2014 / Accepted: 23 February 2015 / Published online: 3 March 2015

Abstract Indium is an essential element in the manufacture of liquid crystal displays and other electronic devices, and several forms of indium compounds have been developed, including nanopowders, films, nanowires, and indium metal complexes. Although there are several reports on lung injury caused by indium-containing compounds, the toxicity of nanoscale indium oxide (In_2O_3) particles has not been reported. Here, we compared lung injury induced by a single exposure to In_2O_3 nanoparticles (NPs) to that caused by benchmark high-toxicity nickel oxide (NiO) and copper oxide (CuO) NPs. In_2O_3 NPs at doses of 7.5, 30, and 90 cm^2/rat (50, 200, and 600 μg/rat) were administered to 6-week-old female Wistar rats via pharyngeal aspiration, and lung inflammation was evaluated 1, 3, 14, and 28 days after treatment. Neutrophilic inflammation was observed on day 1 and worsened until day 28, and severe pulmonary alveolar proteinosis (PAP) was observed on post-aspiration days 14 and 28. In contrast, pharyngeal aspiration of NiO NPs showed severe neutrophilic inflammation on day 1 and lymphocytic inflammation with PAP on day 28. Pharyngeal aspiration of CuO NPs showed severe neutrophilic inflammation on day 1, but symptoms were completely resolved after 14 days and no PAP was observed. The dose of In_2O_3 NPs that produced progressive neutrophilic inflammation and PAP was much less than the doses of other toxic particles that produced this effect, including crystalline silica and NiO NPs. These results suggest that occupational exposure to In_2O_3 NPs can cause severe lung injury.

Keywords Indium oxide · In_2O_3 · Pharyngeal aspiration · Pulmonary alveolar proteinosis · Neutrophilic inflammation · Fibrosis

Introduction

Indium oxide (In_2O_3) nanoparticles (NPs) and indium compounds are widely used in electronics, including sensing devices and liquid crystal displays (LCDs), because of their high electronic conductivity, transparency, and mechanical resistance (Lee et al. 2011; Choi et al. 2012; Elouali et al. 2012). Various forms of In_2O_3 have been developed, including nanopowders, films, nanowires, and indium metal complexes (Zou et al. 2013; Samedov et al. 2012). As the use of In_2O_3 has increased along with its production, concerns about In_2O_3 exposure have grown, particularly with regard to occupational exposure via inhalation of its particulate form. Indeed, 10 clinical cases of lung diseases caused by occupational exposure to indium compounds have been reported in Japan, the USA, and China (Omae et al. 2011). Although several studies have evaluated lung injury produced by indium-containing particles, the toxicity of In_2O_3 NPs is not well understood (Cummings et al. 2012; Lim et al. 2014).

Occupational inhalation exposure to micron-sized In_2O_3 particles is associated with a novel lung disease

Electronic supplementary material The online version of this article (doi:10.1007/s00204-015-1493-x) contains supplementary material, which is available to authorized users.

J. Jeong · J. Kim · W.-S. Cho (✉)
Laboratory of Toxicology, Department of Medicinal Biotechnology, School of Natural Resources and Life Sciences, Dong-A University, 840 Hadan-2dong, Saha-gu, Pusan 604-714, Korea
e-mail: wcho@dau.ac.kr

S. H. Seok
Department of Microbiology and Immunology, Institute of Endemic Disease, Seoul National University College of Medicine, Seoul, Korea

consisting of pulmonary alveolar proteinosis (PAP), granulomas, pulmonary fibrosis, emphysema, and pneumothoraces (Choi et al. 2013; Cummings et al. 2010). PAP is a surfactant accumulation disease in the alveoli that can be occurred by inhalation of several types of dust, including cement dust, silica, and TiO_2 (McCunney and Godefroi 1989; Lee et al. 1986; Sauni et al. 2007). Our recent studies showed that a single exposure to NiO or Co_3O_4 NPs can produce PAP after 4 weeks (Cho et al. 2010, 2012). PAP can be produced by not only proliferation of alveolar type II cells, which release surfactant, but also inhibition of surfactant clearance (Uchida et al. 2007). Because NPs are deposited in the alveoli at a greater rate and easily taken up into cells than bulk particles, NPs are more likely to cause PAP.

Like traditional noxious particles such as crystalline silica and asbestos, manufactured nanomaterials such as NiO, Co_3O_4, and carbon nanotubes show progressive lung injuries such as chronic inflammation, fibrosis, and cancer (Wagner 1997; Cho et al. 2012; Castranova et al. 2013). In addition, delayed-type hypersensitivity-like inflammation caused by NiO and Co_3O_4 NPs might be an emerging pathological pattern in the field of particle toxicology (Cho et al. 2012). Because NPs can produce unknown toxicities as described above, systematic investigation of the toxicity of In_2O_3 NPs is important for hazard identification and development of related industry. In this study, we investigated the pattern of lung injury induced by In_2O_3 NPs at different time-points after NP exposure, and In_2O_3-induced lung injury was compared with injury caused by benchmark high-toxicity nickel oxide (NiO) and copper oxide (CuO) NPs.

Materials and methods

Physicochemical characterization of NPs

A panel of NPs was consisted of In_2O_3 NPs (Nanostructured & Amorphous Materials, Houston, TX, USA) and two representative toxic NPs, NiO NPs (Nanostructured & Amorphous Materials) and CuO NPs (NanoScale, Manhattan, KS, USA), which were selected as benchmark NPs. NP surface area (SA) was measured by the Brunauer–Emmett–Teller (BET) method using a TriStar 3000 SA analyzer (Micromeritics Instrument Corporation, Norcross, GA, USA). The primary size of NPs was measured by transmission electron microscopy (TEM; JEM-1200EX II, JEOL, Tokyo, Japan). The mean size was obtained by counting a minimum of 200 separate NPs. A Zetasizer Nano ZS (Malvern, Malvern Hills, UK) was used to measure the hydrodynamic size, polydispersity, and zeta potential of the NPs in distilled water (DW) according to the manufacturer's instructions. The presence of endotoxins was measured in NPs dispersed in sterile saline at 360 cm^2/mL, which is equivalent to a dose of 90 cm^2/rat, using an endpoint chromogenic *Limulus* amebocyte lysate (LAL) assay (Cambrex, Walkersville, MD, USA). The detection limit of the LAL kit was 0.1–1.0 EU/mL.

Solubility test

To evaluate the stability of NPs, they were incubated with artificial lysosomal fluid (pH 5.5) (Stopford et al. 2003) or 0.9 % saline. NPs at 1 mg/mL were dispersed in each solution and incubated for 1 or 28 days, after which particle-free supernatants were prepared by three rounds of centrifugation at 15,000×*g* for 30 min. Concentrations of indium, copper, and nickel ions in each NP-free supernatant were measured by the Center for Collaborative Instruments at Dong-A University using inductively coupled mass spectrometry (ICP-MS; Agilent Technologies, Seoul, Korea). The dissolved fraction was calculated for each NP by dividing the detected ion mass by the initial mass and expressed as a percentage.

Cell-free reactive oxygen species (ROS) assay

The intrinsic capability of NPs in generating radical electron was measured by 2′7′-dichlorofluorescin diacetate (DCFH-DA), which can detect reactive oxygen species (ROS). The cell-free ROS assay was performed according to the previously described method (Rushton et al. 2010). Briefly, one part of 5 mM DCFH-DA (Calbiochem, La Jolla, CA, USA) in ethanol was deacetylated by addition of 40 parts of sodium hydroxide (0.01 N) for 30 min at room temperature and then neutralized by addition of 200 parts of phosphate-buffered saline (PBS, 25 mM, pH 7.2). Horseradish peroxidase (Sigma-Aldrich, St. Louis, MO, USA) at a final concentration of 2.2 U/mL was added to the mixture. NPs were dispersed in 10 mM PBS (pH 7.4) at concentrations of 20, 60, and 180 cm^2/mL. The mixture and NP suspension were mixed 1:1 and incubated at 37 °C for 15 min and centrifuged at 15,000×*g* for 15 min to collect NP-free supernatant. Therefore, the final concentrations of NPs were 10, 30, and 90 cm^2/mL. The fluorescence intensity was quantified at an excitation wavelength of 485 nm and emission wavelength of 590 nm using a plate reader (Synergy HT Multi-Mode Microplate Reader, Bio-Tek Instruments, Inc., Winooski, VT, USA). Hydrogen peroxide (H_2O_2, Sigma-Aldrich) at 0, 0.625, 1.25, 2.5, 5, and 10 μM was used as a standard curve, and the potential for ROS generation by NP was expressed as H_2O_2 equivalents.

Particle suspension

For in vivo experiments, NPs were prepared and treated based on the SA dose metric because SA has been proposed as an appropriate dose metric for NPs in lung inflammation model (Duffin et al. 2007). For in vivo experiments, the stock solutions of NPs at 3000 cm^2/mL in DW were sonicated using a water bath sonicator (Saehan-Sonic, Seoul, Korea) for 10 min to breakup agglomerations, and working solutions of NPs used to administer 7.5, 30, and 90 cm^2/rat were made using sterile 0.9 % saline. NPs were then sonicated for 5–10 min in a water bath sonicator (Saehan-Sonic). Particle suspensions were prepared immediately before use and vortexed vigorously immediately before each aspiration to minimize NP agglomeration, as recommended by a previous study (Lison et al. 2009).

Administration of NPs to rats via pharyngeal aspiration

Six-week-old specific pathogen-free female Wistar rats were purchased from Samtako (Gyeonggi-do, Korea) and acclimatized for 1 week before the study. Rats were housed in polycarbonate cages with controlled temperature (21–23 °C), humidity (38–55 %), and lighting (12-h light/dark cycle). Water and feed (LabDiet 5002, PMI nutrition, Richmond, IN, USA) were supplied ad libitum. Animals were handled and treated according to policies approved by the Institutional Animal Care and Use Committee of Dong-A University. Rats were randomly assigned to each group, and oral pharyngeal aspiration was performed using previously described methods with slight modifications (Sarlo et al. 2009). Briefly, rats were anesthetized by intraperitoneal injection of tiletamine–zolazepam (Zoletil®, 20 mg/kg) and xylazine (2 mg/kg). Rats were placed on a board in a near-vertical position, and the tongue was gently held at full extension, while 250 µL of the NP suspension was loaded onto the base of the tongue. The tongue was held extended, and the nose was covered to stimulate the gasp reflex until the NP suspension was fully aspirated. As a vehicle control, 250 µL of sterile saline was aspirated. All rats survived the exposure procedure. To evaluate the dose dependency of the effect of In_2O_3 NPs, In_2O_3 NPs were aspirated at 7.5, 30, and 90 cm^2/rat (50, 200, and 600 µg/rat), while NiO NPs were administered as a benchmark NP at 90 cm^2/rat (98.1 µg/rat), and inflammatory responses were evaluated at day 1 or 28 post-aspiration. To evaluate the time-course of the effects, In_2O_3 NPs, along with CuO NPs as a benchmark NP in a separate group, were aspirated at 90 cm^2/rat (600 µg/rat for In_2O_3 and 309 µg/rat for CuO) and lung inflammation and pathological changes were evaluated on post-aspiration days 1, 3, 14, and 28. All animals were observed daily for clinical signs and mortality.

Preparation of BAL fluid

Rats were euthanized by intraperitoneal injection of tiletamine–zolazepam (Zoletil®, 50 mg/kg) and xylazine (5 mg/kg). The trachea was cannulated with a blunt 14 gauge needle, and the lungs were lavaged in situ four times with cold sterile saline at a volume of 8 mL. The first lavage was kept for separate analysis, and cell pellets from each lavage were pooled for cell counts. The total number of cells in the BAL fluid was quantified by hemocytometric counting, and cells were attached to slide glasses by spinning them with a cytospin centrifuge at $15\times g$ for 5 min. The slides were dried, fixed with methanol, and stained with Diff-Quik (Thermo Fisher Scientific, Waltham, MA, USA) for differential cell counting.

Analysis of BAL fluid

Differential cell counts were performed by counting a minimum of 300 cells under a light microscope (Nikon, Tokyo, Japan). Lactate dehydrogenase (LDH), a cytotoxicity marker, was measured in BAL fluid using an LDH assay kit according to the manufacturer's instructions (Roche Diagnostics, Mannheim, Germany). Total protein, a marker for vascular permeability, was measured in the BAL fluid using a bicinchoninic acid (BCA) assay kit (Thermo Fisher Scientific, Waltham, MA, USA). Proinflammatory cytokines interleukin-1β (IL-1β), IL-2, IL-6, IL-10, cytokine-induced neutrophil chemoattractant-3 (CINC-3), and tumor necrosis factor-α (TNF-α) were measured in non-diluted BAL fluid using Duoset ELISA kits (R&D systems, Minneapolis, MN, USA). The concentrations of phospholipids, which are major components of pulmonary surfactant, were measured in BAL fluid using a phospholipid assay kit (Bioassay systems, Hayward, CA, USA).

Histological analysis

Lung tissues from rats were prepared and stained with hematoxylin and eosin (H&E) as previously described (Cho et al. 2012). Routine periodic acid-Schiff staining (PAS; Merk KGaA, Darmstadt, Germany) was performed on lung tissue sections to detect glycoprotein accumulation. Pulmonary fibrosis was evaluated by staining collagen with picrosirius red stain (PSR; Sigma-Aldrich) according to the manufacturer's instructions.

Immunohistochemistry for Ki-67

Paraffin-embedded lung tissue samples were sectioned, dewaxed, and hydrated using a xylene–alcohol series. H_2O_2 (3 %) was applied for 15 min to quench the endogenous

peroxidase, and antigen retrieval was performed by microwaving the sections for 30 min in Tris–EDTA buffer (10 mM Tris base, 1 mM EDTA solution, 0.05 % Tween 20, pH 9.0). After blocking the section with normal goat serum (Vectastain® ABC kit; Vector Laboratories, Burlingame, CA, USA), the Ki-67 monoclonal antibody (clone SP6; Abcam, Cambridge, UK) was applied at a 1:100 dilution for 1 h at room temperature. After washing the section with PBS containing 0.025 % Triton X-100, biotinylated secondary antibody and Vectastain® ABC reagent were applied according to the manufacturer's instructions (Vector Laboratories). DAB (3,3′-diaminobenzidine) substrate solution (Vector Laboratories) was applied for about 10 min and rinsed off with tap water before the sections were counterstained with Mayer's hematoxylin (Dako, Glostrup, Denmark).

Treatment of NPs to primary cultured rat alveolar macrophages

To evaluate the mechanism of toxicity by In_2O_3 NPs, alveolar macrophages were collected from 6-week-old female Wistar rats as previously described method (Cho et al. 2013). The collected cells were then cultured in 96-well plates (Nunc, Roskilde, Denmark) at a density of 1×10^6 cells/mL in RPMI 1640 (Life Technologies, Grand Island, NY, USA) containing 10 % fetal bovine serum (Life Technologies), 2 mM L-glutamine (Life Technologies), 100 IU/mL penicillin, and 100 IU/mL streptomycin (Life Technologies). After 4-h incubation at 37 °C with 5 % CO_2, cells were washed with pre-warmed PBS and treated with In_2O_3 NPs at 30, 100, and 300 cm^2/mL or CuO NPs at 3, 10, and 30 cm^2/mL based on the dose-range finding study. NPs were treated for 24 h, and cytotoxicity and pro-inflammatory cytokine expression was evaluated. Trypan blue exclusion assay was performed to evaluate the cytotoxicity, and pro-inflammatory cytokines including IL-1β, IL-6, and CINC-3 were measured in the cell culture supernatant using commercial ELISA kits (all from R&D systems).

Statistical analysis

Data were analyzed with GraphPad Prism software (ver. 6.0, La Jolla, CA, USA). Each treatment group was compared with the vehicle control group by one-way analysis of variance (ANOVA) with Tukey's range test for pairwise post hoc comparisons. A result of $p < 0.05$ was considered to be statistically significant.

Results

Physicochemical properties of NPs

The physicochemical properties of the NPs used in this study are summarized in Table 1, and the representative TEM images of NPs are presented in Supplemental Fig. S1. The primary size of the In_2O_3 NPs was 35.8 ± 1.1 nm, while the hydrodynamic size was 212.7 ± 2.2 nm, which indicated that the NPs were agglomerated. The NiO and CuO NPs showed agglomeration similar to that observed in the In_2O_3 NPs, and those agglomerations were soft agglomerations which can be easily dispersed by simple sonication. All NPs showed <4 % dissolution in saline after 28 days of incubation, while their solubility in acidic artificial lysosomal fluid (ALF, pH 5.5) was variable; CuO NPs were most soluble in ALF, followed by NiO NPs, and In_2O_3 NPs were least soluble. All NPs showed positive zeta potentials greater than +37 mV when they were dispersed in DW. The LAL assay showed that endotoxins were below the detection limit in all NPs.

Table 1 Physicochemical characterization of NPs

NPs	In_2O_3	NiO	CuO
Primary size (nm)	35.8 ± 1.1[a]	5.3 ± 1.9	23.1 ± 7.2
Surface area (m^2/g)	15	91.8	29
Hydrodynamic size (nm) in DW	212.7 ± 2.2	209.7 ± 3.7	171.7 ± 1.6
Polydispersity in DW	0.13 ± 0.01	0.30 ± 0.02	0.17 ± 0.02
Solubility (%) in saline at			
Day 1	1.1	1.1	0.51
Day 28	3.3	3.3	1.0
Solubility (%) in ALF at			
Day 1	0.6	9.5	97.3
Day 28	5.5	42.3	100
Zeta potential (mV) in DW	+57.2 ± 0.5	+48.9 ± 0.6	+37.4 ± 0.7
Mass (μg) for 90 cm^2	600	98.1	309

DW distilled water, *ALF* artificial lysosomal fluid

[a] Data were presented as mean ± SD

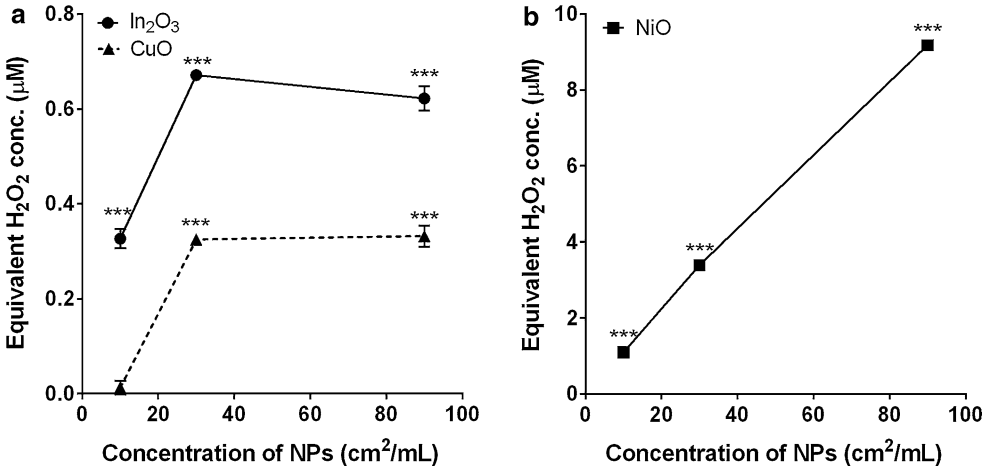

Fig. 1 Cell-free ROS activity of NPs using DCFH-DA fluorescence assay. Data are expressed as H_2O_2 equivalent activity. Values are mean ± SD ($n = 4$) for each treatment group. Each treatment group was compared with the vehicle control (PBS) to determine statistical significance. ***$p < 0.001$

Cell-free ROS generation potential of NPs

Although the potential for generation of ROS was different each NP, all NPs tested in this study showed significant increases compared to vehicle control (Fig. 1). In_2O_3 and CuO NPs showed mild increases with saturation at 30 cm^2/mL, while NiO NPs showed massive increases in the ROS generation, which was above tenfold higher than those of In_2O_3 and CuO NPs.

Lung inflammation after pharyngeal aspiration of In_2O_3 and NiO NPs

On post-aspiration day 1, In_2O_3 NPs did not significantly increase total cell number or differential cell count, while NiO NPs significantly increased the total number of cells and polymorphonuclear leukocytes (PMN) (Fig. 2a–d). In_2O_3 NPs produced PMN abundance significantly greater than that of the vehicle-treated group, and In_2O_3 and NiO NPs at 90 cm^2/rat produced dose-dependent increases in the abundance of PMN, which accounted for 27.5 ± 14.8 and 46.2 ± 14.4 % of the total cells, respectively.

On post-aspiration day 28, In_2O_3 NPs significantly increased the number of total cells, macrophages, and PMN, while NiO NPs significantly increased the number of lymphocytes (Fig. 2e–h). Although the number of PMN in the NiO NP-treated group was not significantly different from the number in the vehicle-treated control group, PMN accounted for 22.0 ± 7.3 % of the total cells from the group treated with NiO NP at 90 cm^2/rat (Table 2). In_2O_3 NPs showed dose-dependent effects and markedly increased PMN recruitment compared to that observed on post-aspiration day 1; In_2O_3 NPs at 7.5 cm^2/rat were not inflammogenic on post-aspiration day 1, but led to recruitment of 12.5 ± 2.0 × 10^6 PMN on post-aspiration day 28, which represented 81.3 ± 6.9 % of the total cells (Table 2). There were no observable clinical signs in all treatment groups although In_2O_3 and NiO NPs caused progressive lung injury.

Cytotoxicity and total protein levels in BAL fluid after aspiration of In_2O_3 and NiO NPs

On post-aspiration day 1, LDH levels in the In_2O_3 NP-treated groups were comparable to those of the vehicle control group, but were markedly increased in a dose-dependent manner on post-aspiration day 28 (Fig. 3a, b). LDH levels in the NiO NPs-treated groups were significantly increased at both time-points. For groups treated with In_2O_3 and NiO NPs, LDH levels on post-aspiration day 28 were much greater than those observed on post-aspiration day 1. On post-aspiration day 1, the total protein concentration in In_2O_3 NPs showed significant increase only in the high-dose group (Fig. 3c). However, In_2O_3 NPs showed higher levels of total protein with clear dose dependency at day 28 in comparison with day 1 (Fig. 3c, d). NiO NPs significantly increased total protein level at both time-points.

Levels of phospholipids in BAL fluid after pharyngeal aspiration of In_2O_3 and NiO NPs

On post-aspiration day 1, In_2O_3 and NiO NPs produced slight increases in phospholipid levels, which were <100 μM in all treatment groups (Fig. 4a). However, with the exception of the lowest tested dose (7.5 cm^2/rat), all NP treatments produced levels of phospholipids >2000 μM on post-aspiration day 28, and the effects of the In_2O_3 NPs were dose dependent (Fig. 4b).

Pro-inflammatory cytokines in BAL fluid after pharyngeal aspiration of In_2O_3 and NiO NPs

On post-aspiration day 1, In_2O_3 NPs significantly increased the abundance of CINC-3, while NiO NPs significantly

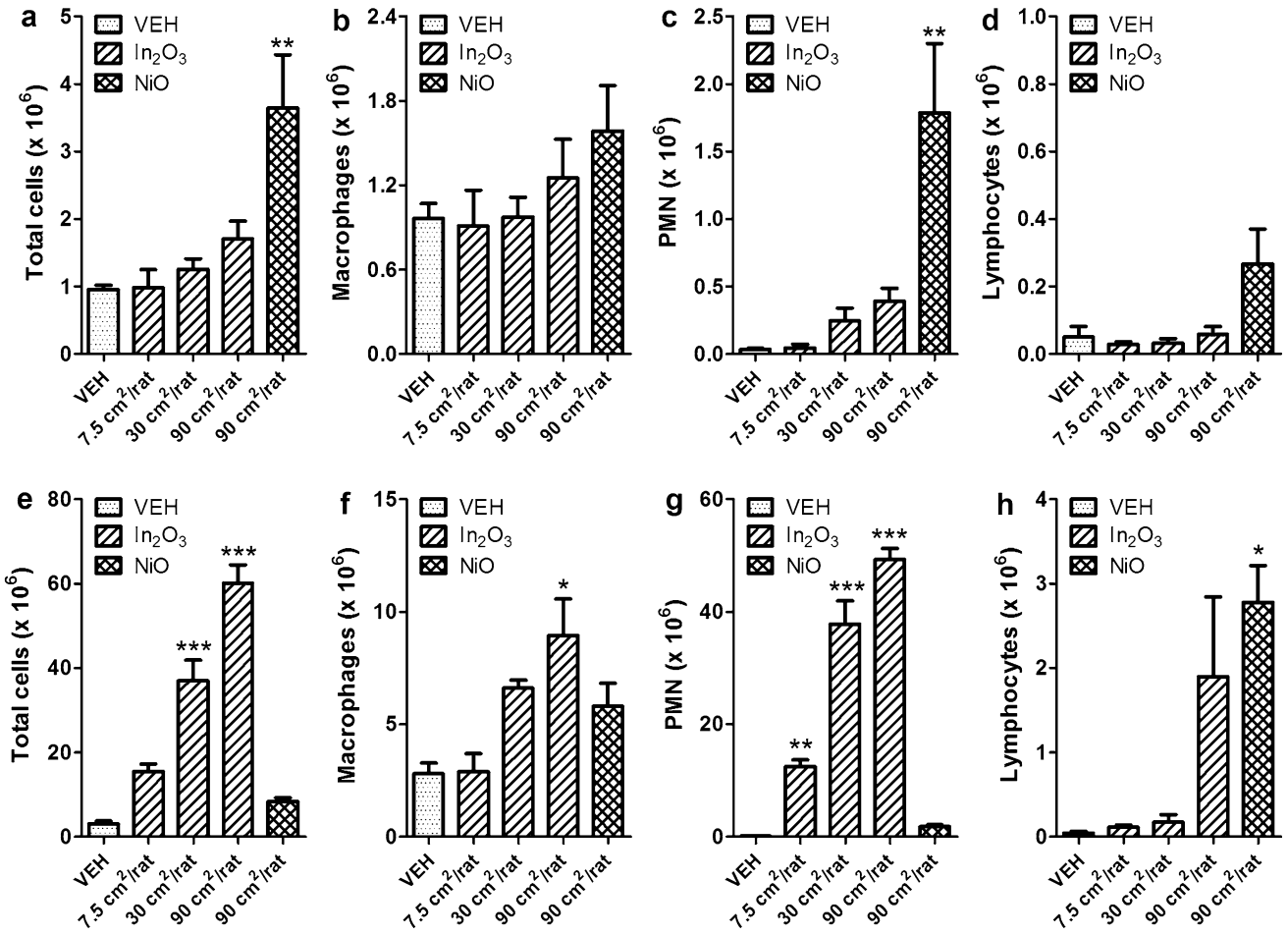

Fig. 2 Differential cell counts in bronchoalveolar lavage (BAL) fluid at day 1 or 28 after pharyngeal aspiration of In_2O_3 NPs or NiO NPs. Number of **a** total cells, **b** macrophages, **c** polymorphonuclear leukocytes (PMN), and **d** lymphocytes on post-aspiration day 1. Number of **e** total cells, **f** macrophages, **g** PMN, and **h** lymphocytes on post-aspiration day 28. Values are mean ± SD ($n = 4$) for each treatment group. Each treatment group was compared with the vehicle control (VEH) group to determine statistical significance. $^*p < 0.05$; $^{**}p < 0.01$; $^{***}p < 0.001$

Table 2 Percentage of differential cells in BAL fluid

	Macrophages (%)	PMN (%)	Lymphocytes (%)
24 h after pharyngeal aspiration			
Vehicle control	93.6 ± 0.9	4.1 ± 1.3	2.3 ± 2.4
In_2O_3 (7.5 cm^2/rat)	92.7 ± 5.5	4.4 ± 4.7	2.8 ± 0.8
In_2O_3 (30 cm^2/rat)	78.4 ± 13.3	19.2 ± 12.3	2.4 ± 1.9
In_2O_3 (90 cm^2/rat)	70.7 ± 14	25.8 ± 14.7	3.4 ± 2.0
NiO (90 cm^2/rat)	47.1 ± 13.7***	46.2 ± 14.3***	6.6 ± 3.9
4 weeks after pharyngeal aspiration			
Vehicle control	89.6 ± 4.1	4.5 ± 1.5	5.9 ± 2.6
In_2O_3 (7.5 cm^2/rat)	17.9 ± 6.7***	81.3 ± 6.9***	0.7 ± 0.2
In_2O_3 (30 cm^2/rat)	15.0 ± 3.0***	84.7 ± 2.5***	0.3 ± 0.5
In_2O_3 (90 cm^2/rat)	14.5 ± 3.3***	82.5 ± 5.1***	2.9 ± 2.6
NiO (90 cm^2/rat)	68.6 ± 11.8**	22.0 ± 7.3**	9.2 ± 8.1

Values are mean ± SD ($n = 4$) for each treatment group. Each treatment group was compared with the vehicle control group to determine statistical significance

** $p < 0.01$

*** $p < 0.001$

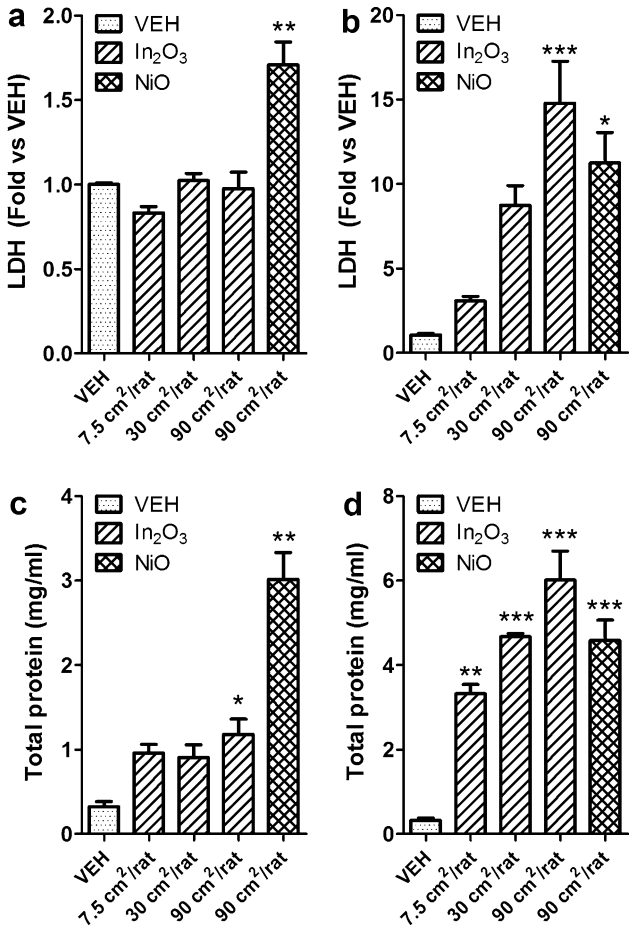

Fig. 3 Levels of lactate dehydrogenase (LDH) and total protein in bronchoalveolar lavage (BAL) fluid at day 1 or 28 after pharyngeal aspiration of In_2O_3 NPs or NiO NPs. Levels of LDH on **a** post-aspiration day 1 and **b** 28. Levels of total protein on **c** post-aspiration day 1 and **d** 28. Levels of LDH and total protein on post-aspiration day 28 were much higher than those on post-aspiration day 1. Values are mean ± SD ($n = 4$) for each treatment group. Each treatment group was compared with the vehicle control (VEH) group to determine statistical significance. *$p < 0.05$; **$p < 0.01$; ***$p < 0.001$

increased the abundance of IL-1β, CINC-3, and TNF-α (Fig. 5). However, IL-2, IL-6, and IL-10 were not significantly changed by any NP treatment (Supplemental Table S1). Pro-inflammatory cytokines showed no statistical changes by any treatment on post-aspiration day 28 (Supplemental Table S1).

Evaluation of the time-course of inflammation produced by In_2O_3 and CuO NPs

To evaluate the time-course of inflammation produced by In_2O_3 NPs, rats were killed 1, 3, 14, and 28 days after a single aspiration. As a benchmark, the inflammation produced by CuO NPs was compared with that produced by In_2O_3 NPs. In_2O_3 NPs showed mild neutrophilic inflammation on post-aspiration days 1 and 3, while progressive neutrophilic inflammation was evident on post-aspiration days 14 and 28 (Fig. 6a). In contrast, CuO NPs showed severe acute inflammation on post-aspiration day 1, which was not resolved until day 14. The detail cell counts were presented in the Supplemental Table S2. Phospholipid measurements showed that In_2O_3 NPs produced PAP by post-aspiration day 14 that was maintained through post-aspiration day 28, while CuO NPs did not significantly increase phospholipid levels (Fig. 6b). In consistent with the inflammatory response, rats treated with CuO NPs showed depression with reduction in water and feed intake at days 1 and 3, while the clinical signs were recovered thereafter.

Histological analysis and immunohistochemistry of Ki-67 in lungs exposed to In_2O_3 NPs

On post-aspiration day 1, In_2O_3 NPs produced multifocal mild-to-moderate neutrophil aggregates, which were consistent with the BAL fluid analysis (Fig. 7b). On post-aspiration day 28, In_2O_3 NPs produced severe multifocal granulomatous inflammation in the perivascular regions, as well as in the alveoli (Fig. 7c, d). Foamy macrophages and neutrophils infiltrated the alveoli, and homogenous eosinophilic materials were deposited, which were identified as glycoproteins via PAS staining (Fig. 7d; Supplemental Fig. S1). PSR staining showed that In_2O_3 NPs did not produce fibrotic lesions (Supplemental Fig. S2). Immunohistochemistry for Ki-67 in the lungs on post-aspiration day 28 showed that In_2O_3 NPs increased the number of Ki-67-positive cells, which mainly consisted of alveolar type II-like cells (Fig. 8).

Cytotoxicity and pro-inflammatory cytokines expression in rat alveolar macrophages

Both In_2O_3 and CuO NPs induced significant cell death, but CuO NPs showed higher cytotoxicity than In_2O_3 NPs based on trypan blue exclusion assay (Fig. 9a). Treatment of In_2O_3 NPs to rat alveolar macrophages showed significantly increased levels of IL-1β, IL-6, and CINC-3, while CuO NPs showed no significant increases (Fig. 9b–d).

Discussion

Indium compounds are essential elements in various industrial applications, including the manufacture of LCD screens and other electronic devices, and indium production volume has exponentially increased during the past 5 years (Cummings et al. 2012). As the need for indium compounds has increased, nanoscale indium compounds have been applied in microelectronic devices because their small size can improve performance (Seo et al. 2003; Murali et al. 2001).

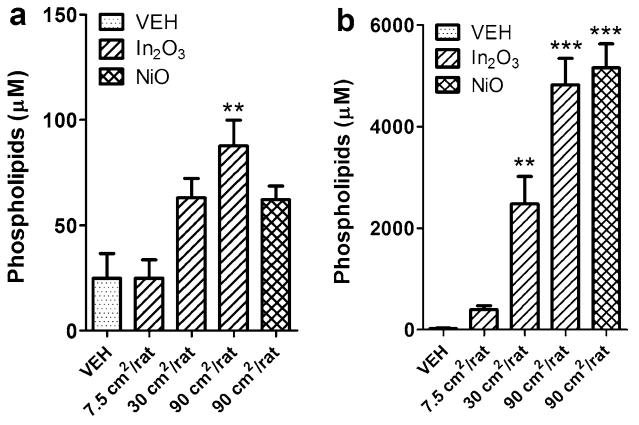

Fig. 4 Levels of phospholipids in bronchoalveolar lavage (BAL) fluid at day 1 or 28 after pharyngeal aspiration of In_2O_3 NPs or NiO NPs. **a** Levels of phospholipids on post-aspiration day 1 were slightly increased by In_2O_3 NPs. **b** Levels of phospholipids on post-aspiration day 28 produced by In_2O_3 NPs and NiO NPs were much higher than levels on post-aspiration day 1. Values are mean ± SD ($n = 4$) for each treatment group. Each treatment group was compared with the vehicle control (VEH) group to determine statistical significance. $^{**}p < 0.01$; $^{***}p < 0.001$

Increased needs and production volume of indium compounds may lead higher risk to human exposure mainly in occupational settings. Occupational inhalation exposure to indium compounds has been shown to cause indium lung disease, which is characterized by pulmonary fibrosis, emphysema, and PAP (Cummings et al. 2012). However, little is known regarding the hazard to human health posed by In_2O_3, a nano-particulate indium form.

Pharyngeal aspiration of In_2O_3 NPs in this study showed mild neutrophilic inflammation on post-aspiration day 1, which continuously worsened, and severe neutrophilic inflammation and PAP were observed from post-aspiration day 14. Lung injury produced by In_2O_3 NPs was contrasted with that produced by NiO NPs, which showed severe neutrophilic inflammation on post-aspiration day 1 and lymphocytic inflammation with PAP on post-aspiration day 28 (Cho et al. 2010, 2012; Mizuguchi et al. 2013). The acute severe neutrophilic inflammation associated with CuO NPs is thought to be produced by fast dissolution in the acidic lysosomal fluid, and this dissolution can result in fast NP clearance and a low incidence of chronic lung injury (Zhang et al. 2012). In previous studies, the potential for ROS generation by NPs was reported as a main mechanism for the acute lung inflammation (Rushton et al. 2010; Han et al. 2012). Interestingly, the low potential for ROS generation of In_2O_3 NPs and the high potential for ROS generation of NiO NPs were consistent with the low and high inflammatory potential at 24 h of In_2O_3 and NiO NPs, respectively.

Acute neutrophilic inflammation produced by In_2O_3 NPs on post-aspiration day 1 was mediated by CINC-3, rather than by IL-1β, IL-2, IL-6, IL-10, or TNF-α, while no significant changes were found on post-aspiration day 28, although inflammation in the lung at this time-point was much worse than that observed on post-aspiration day 1. The lack of significant increases in pro-inflammatory cytokine levels on post-aspiration day 28 was consistent with a previous study using micron-sized indium–tin–oxide (ITO) particles, which reported ITO-induced severe lung inflammation, but no significant increase in TNF-α in the BAL fluid (Lison et al. 2009). In addition, In_2O_3 NPs induced levels of cytokines lower than those induced by NiO NPs on post-aspiration day 1, which was consistent

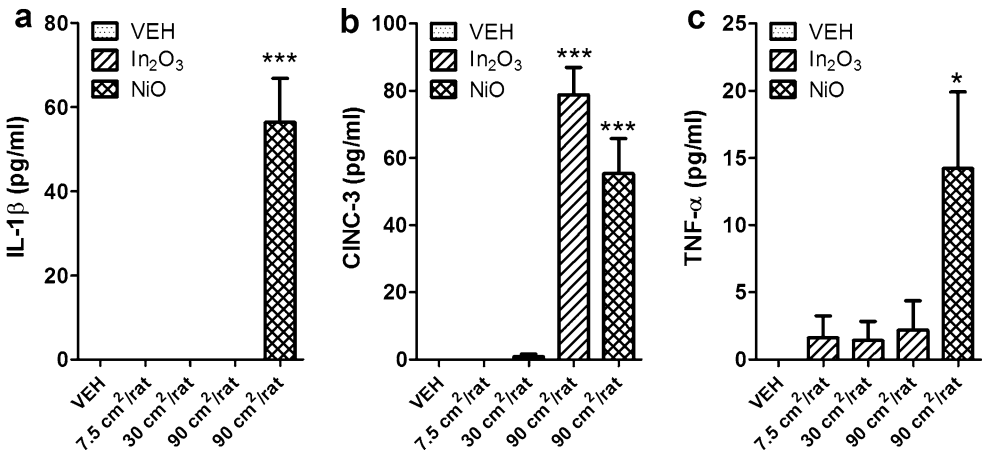

Fig. 5 Pro-inflammatory cytokines in the bronchoalveolar lavage (BAL) fluid at day 1 after pharyngeal aspiration of In_2O_3 NPs or NiO NPs. Levels of **a** IL-1β, **b** CINC-3, and **c** TNF-α were significantly increased by NiO NPs, while levels of CINC-3 were significantly increased by In_2O_3 NPs at a dose of 90 cm^2/rat. Values are mean ± SD ($n = 4$) for each treatment group. Each treatment group was compared with the vehicle control (VEH) group to determine statistical significance. $^{*}p < 0.05$; $^{***}p < 0.001$

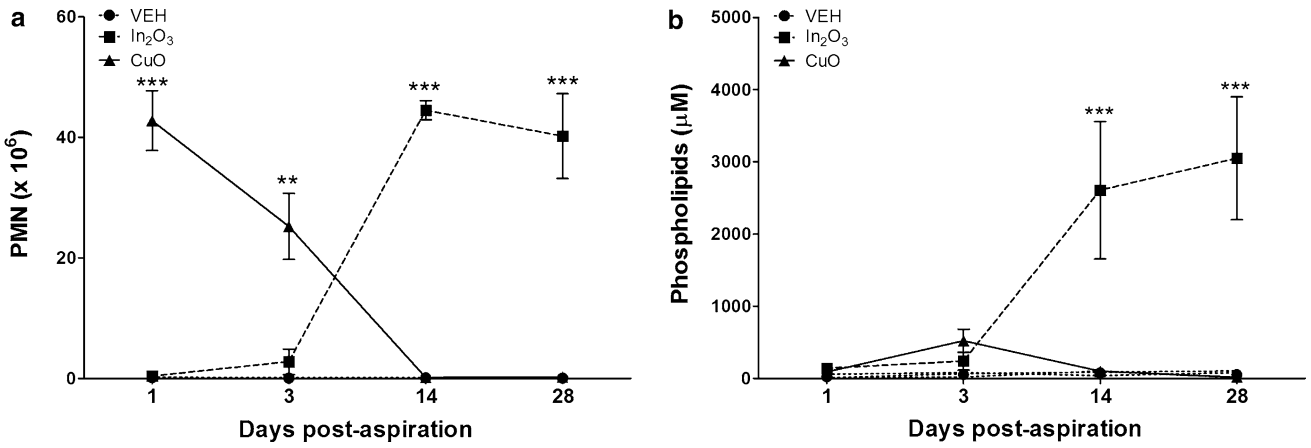

Fig. 6 Time-course of lung injury in rats treated with In_2O_3 and CuO NPs at a dose of 90 cm^2/rat. **a** In_2O_3 NPs produced a continuous increase in polymorphonuclear leukocyte (PMN) abundance, while CuO NPs produced a continuous decrease in this measure. **b** In_2O_3 NPs increased phospholipid levels over time, but phospholipid levels after treatment with CuO NPs were not significantly different from those of the vehicle control (VEH) group. Values are mean ± SD ($n = 4$) for each treatment group. Each treatment group was compared with the VEH group to determine statistical significance. $^{**}p < 0.01$; $^{***}p < 0.001$

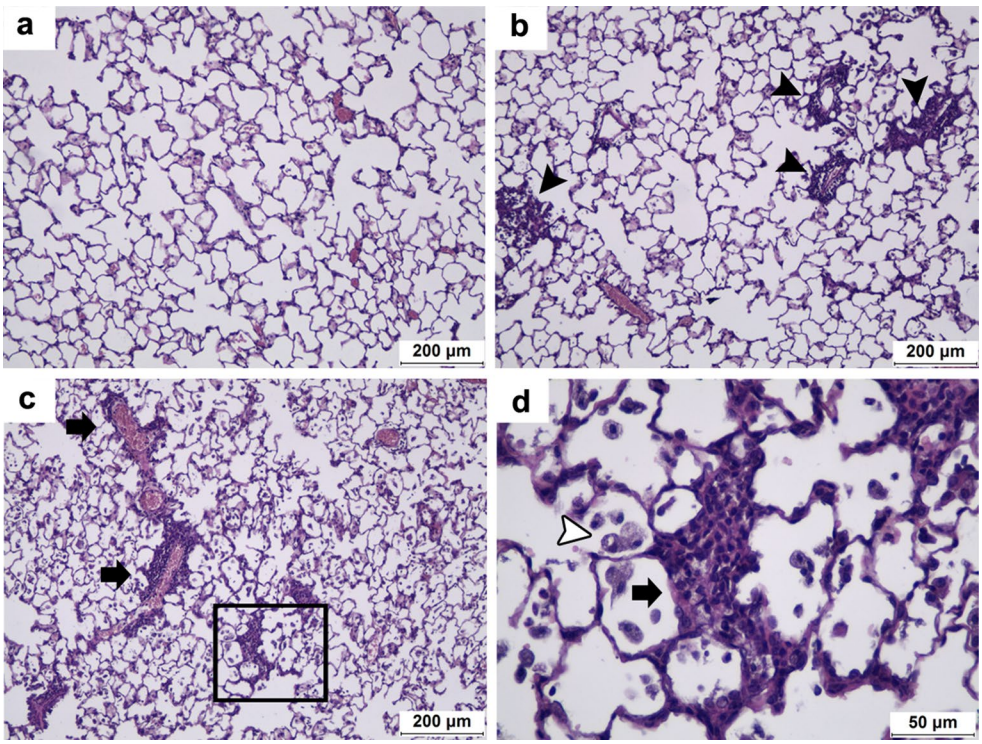

Fig. 7 Representative lung histology after pharyngeal aspiration of In_2O_3 NPs at a dose of 90 cm^2/rat. **a** Normal lung histology of the vehicle control group on post-aspiration day 1. **b** In_2O_3 NPs showed mild-to-moderate multifocal inflammatory foci (*black arrow heads*) in the lung on post-aspiration day 1. **c**, **d** On post-aspiration day 28, In_2O_3 NPs produced multifocal granulomatous inflammation in the perivascular regions, as well as in the alveoli (*arrows*). **d** The higher magnification *boxed area* in **c** shows granuloma formation in the alveoli (*arrow*) and infiltration of foamy macrophages (*white arrow head*) and neutrophils in the alveoli

with the milder neutrophilic inflammation produced by In_2O_3 NPs during the acute exposure phase.

Treatment with In_2O_3 NPs showed no fibrotic lesions during the 28-day post-aspiration evaluation period, and this result was consistent with that obtained using micron-sized ITO, which showed no fibrotic lesions 60 days after pharyngeal aspiration into rats (Lison et al. 2009). Aspiration of In_2O_3 NPs produced multifocal granulomatous

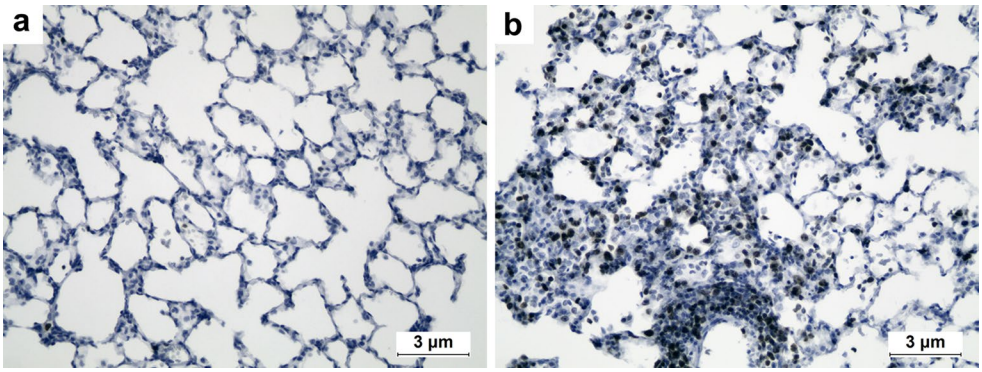

Fig. 8 Immunohistochemistry for Ki-67 in the lungs at day 28 after pharyngeal aspiration of In_2O_3 NPs. **a** Vehicle control on post-aspiration day 28. **b** In the lungs of In_2O_3 NP-treated rats, Ki-67-positive cells were mainly alveolar type II-like cells

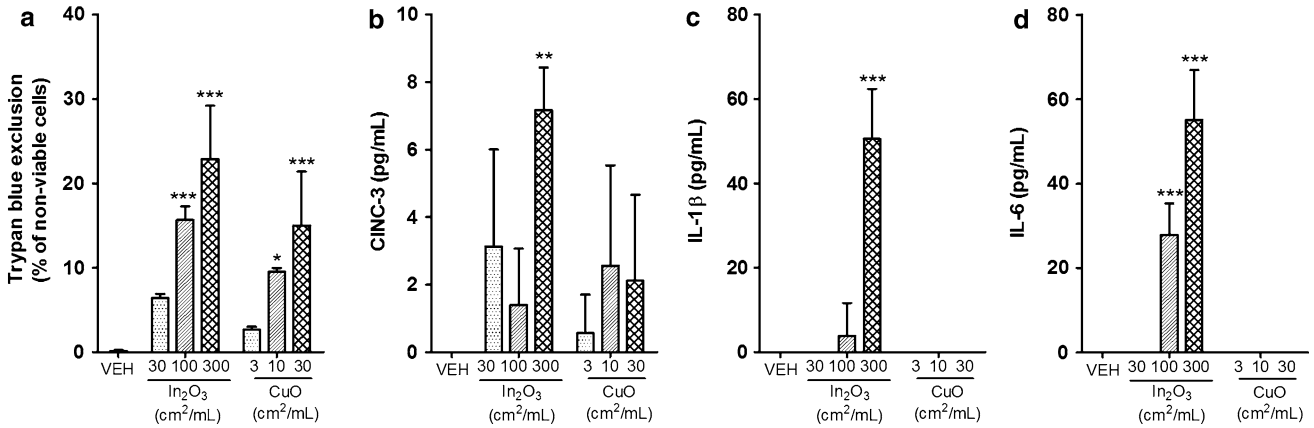

Fig. 9 Cytotoxicity and pro-inflammatory cytokines expression of primary cultured alveolar macrophages by the treatment of In_2O_3 and CuO NPs. **a** Cytotoxicity was measured by trypan blue exclusion assay, **b** CINC-3, **c** IL-1β, **d** IL-6. Values are mean ± SD ($n = 4$) for each treatment group. Each treatment group was compared with the vehicle control (VEH) group to determine statistical significance. $^*p < 0.05$; $^{**}p < 0.01$; $^{***}p < 0.001$

inflammation in the lung on post-aspiration day 28, and this result was consistent with those obtained using ZnO and CuO NPs (Cho et al. 2010). In a previous study, PAP and pulmonary fibrosis were found 1–2 and 4–13 years, respectively, after the subject's first indium exposure (Cummings et al. 2012). Therefore, the observation that PAP was evident from day 14 after a single exposure of rats to In_2O_3 NPs, while no fibrotic lesions occurred until post-aspiration day 28, implies that long-term studies are needed to evaluate the fibrotic potential of In_2O_3 NPs.

We found that PAP was evident from post-aspiration day 14, and proteinaceous materials were localized in the alveolar spaces. PAP can be produced by proliferation of alveolar type II cells, which generate surfactant, or by reducing the abundance of alveolar macrophages, which remove surfactant. Anti-GM-CSF autoantibodies, which reduce the number of alveolar macrophages, can also be used to develop PAP (Uchida et al. 2007). However, in this study, the number of alveolar macrophages was significantly increased by exposure to In_2O_3 NPs. Therefore, autoantibodies against GM-CSF might not be involved in the PAP produced by In_2O_3 NPs. The overproduction of surfactant caused by proliferation of alveolar type II cells might be the main mechanism of PAP induced by In_2O_3 NPs.

In this study, we used female rats, but recent studies showed that there are gender differences in sensitivity of chemical/NP exposure. For chemicals such cadmium, nickel, lead, mercury, and arsenic, gender differences have been reported in the deposition and toxicity, but more affected gender was differed by the types of chemicals (Vahter et al. 2007). Gender differences were also reported for NPs (e.g., silver NPs) in both inhalation and oral exposure settings (Sung et al. 2009; Kim et al. 2010). However, there is little information about the gender effects in the target organ and lung inflammation by NP exposure, which is warranted for further study.

The main target cells were known as alveolar macrophages when aspirated indium phosphide (InP) particles into rodent lung (Kirby et al. 2009). In this study, treatment of In_2O_3 NPs to primary cultured alveolar macrophages induced cell death with stimulation of neutrophil-associated pro-inflammatory cytokines including IL-1β, IL-6, and CINC-3, while CuO NPs caused cell death without stimulating pro-inflammatory cytokines. Therefore, the toxicity by In_2O_3 NPs was induced by the insoluble phagocytosed NPs, which can continuously stimulate inflammatory response, and those toxicity patterns were consistent with the progressive lung injury found in this study. However, cell death without stimulation of pro-inflammatory cytokines might be due to the ionized copper, which is highly toxic to cells.

Our results showed that In_2O_3 NPs produced severe progressive neutrophilic inflammation at doses ≥7.5 cm^2/rat (50 μg/rat), and severe PAP was developed at doses ≥30 cm^2/rat (200 μg/rat). A previous study using micron-sized ITO showed that significant inflammation was produced at doses ≥20 mg/rat after post-aspiration day 15, while PAP was produced at doses ≥2 mg/rat after post-aspiration day 60 (Lison et al. 2009; Lison and Delos 2010). Intratracheal instillation of crystalline silica at 5 mg/kg (about 1.23 mg/rat) showed significant neutrophilic inflammation from day 1 to day 90 after instillation, while instillation of crystalline silica at 1 mg/kg (about 248 μg/rat) showed transient inflammation (Warheit et al. 2006). Intratracheal instillation of coarse CeO_2 (3.9 μm) or fine CeO_2 (0.2 μm) at 10 mg/rat developed PAP (Toya et al. 2010), as did intratracheal instillation of Co_3O_4 NPs (18.4 nm; 419.0 μg/rat) and NiO NPs (5.3 nm; 163.5 μg/rat) (Cho et al. 2012). Therefore, the dose of In_2O_3 NPs required to produce progressive neutrophilic inflammation is much less than that required for other particles, including crystalline silica, and the dose of In_2O_3 NPs required to develop PAP is also much less than that of other particles, including NiO NPs.

In this study, administration of In_2O_3 NPs to rats via pharyngeal aspiration showed progressive neutrophilic inflammation and PAP, which contrasted with the effects of NiO NPs, which produced delayed-type hypersensitivity, and the effects of CuO NPs, which produced acute inflammation with fast resolution. Lung injury produced by In_2O_3 NPs was representative of typical lesions of indium compounds, with the exception of fibrosis and emphysema. Our results indicate that the toxicity of In_2O_3 NPs is comparable to, or higher than, that of most previously studied particles, and thus, In_2O_3 NPs should be grouped with high-toxicity particles such as crystalline silica, NiO NPs, and CuO NPs. In addition, further studies using in vivo and in vitro models are needed to substantiate the results reported in this study.

Acknowledgments Financial support for this study was provided by the Korean Ministry of Food and Drug Safety (13182MFDS606 and 15182MFDS462).

Conflict of interest The authors declare that they have no conflict of interest.

References

Castranova V, Schulte PA, Zumwalde RD (2013) Occupational nanosafety considerations for carbon nanotubes and carbon nanofibers. Acc Chem Res 46(3):642–649

Cho WS, Duffin R, Poland CA, Howie SE, MacNee W, Bradley M, Megson IL, Donaldson K (2010) Metal oxide nanoparticles induce unique inflammatory footprints in the lung: important implications for nanoparticle testing. Environ Health Perspect 118(12):1699–1706

Cho WS, Duffin R, Bradley M, Megson IL, MacNee W, Howie SEM, Donaldson K (2012) NiO and Co_3O_4 nanoparticles induce lung DTH-like responses and alveolar lipoproteinosis. Eur Respir J 39(3):546–557

Cho WS, Duffin R, Bradley M, Megson IL, Macnee W, Lee JK, Jeong J, Donaldson K (2013) Predictive value of in vitro assays depends on the mechanism of toxicity of metal oxide nanoparticles. Part Fibre Toxicol 10(1):55

Choi WS, Kim BJ, Lee HJ, Choi JW, Kim SD, Min NK (2012) Study on the micro-heater geometry in In, 2O3 micro electro mechanical systems gas sensor platforms and effects on NO2 gas detecting performances. J Nanosci Nanotechnol 12(2):1170–1173

Choi S, Won YL, Kim D, Yi GY, Park JS, Kim EA (2013) Subclinical interstitial lung damage in workers exposed to indium compounds. Ann Occup Environ Med 25(1):24

Cummings KJ, Donat WE, Ettensohn DB, Roggli VL, Ingram P, Kreiss K (2010) Pulmonary alveolar proteinosis in workers at an indium processing facility. Am J Respir Crit Care Med 181(5):458–464

Cummings KJ, Nakano M, Omae K, Takeuchi K, Chonan T, Xiao YL, Harley RA, Roggli VL, Hebisawa A, Tallaksen RJ, Trapnell BC, Day GA, Saito R, Stanton ML, Suarthana E, Kreiss K (2012) Indium lung disease. Chest 141(6):1512–1521

Duffin R, Tran L, Brown D, Stone V, Donaldson K (2007) Proinflammogenic effects of low-toxicity and metal nanoparticles in vivo and in vitro: highlighting the role of particle surface area and surface reactivity. Inhal Toxicol 19(10):849–856

Elouali S, Bloor LG, Binions R, Parkin IP, Carmalt CJ, Darr JA (2012) Gas sensing with nano-indium oxides (In_2O_3) prepared via continuous hydrothermal flow synthesis. Langmuir 28(3):1879–1885

Han X, Corson N, Wade-Mercer P, Gelein R, Jiang J, Sahu M, Biswas P, Finkelstein JN, Elder A, Oberdorster G (2012) Assessing the relevance of in vitro studies in nanotoxicology by examining correlations between in vitro and in vivo data. Toxicology 297(1–3):1–9

Kim YS, Song MY, Park JD, Song KS, Ryu HR, Chung YH, Chang HK, Lee JH, Oh KH, Kelman BJ, Hwang IK, Yu IJ (2010) Subchronic oral toxicity of silver nanoparticles. Part Fibre Toxicol 7:20

Kirby PJ, Shines CJ, Taylor GJ, Bousquet RW, Price HC, Everitt JI, Morgan DL (2009) Pleural effects of indium phosphide in B6C3F1 mice: nonfibrous particulate induced pleural fibrosis. Exp Lung Res 35(10):858–882

Lee KP, Henry NW 3rd, Trochimowicz HJ, Reinhardt CF (1986) Pulmonary response to impaired lung clearance in rats following excessive TiO2 dust deposition. Environ Res 41(1):144–167

Lee C, Srisungsitthisunti P, Park S, Kim S, Xu X, Roy K, Janes DB, Zhou C, Ju S, Qi M (2011) Control of current saturation and threshold voltage shift in indium oxide nanowire transistors with femtosecond laser annealing. ACS Nano 5(2):1095–1101

Lim CH, Han JH, Cho HW, Kang M (2014) Studies on the toxicity and distribution of indium compounds according to particle size in sprague-dawley rats. Toxicol Res 30(1):55–63

Lison D, Delos M (2010) Pulmonary alveolar proteinosis in workers at an indium processing facility. Am J Respir Crit Care Med 182(4):578; author reply 578–579

Lison D, Laloy J, Corazzari I, Muller J, Rabolli V, Panin N, Huaux F, Fenoglio I, Fubini B (2009) Sintered indium-tin-oxide (ITO) particles: a new pneumotoxic entity. Toxicol Sci 108(2):472–481

McCunney RJ, Godefroi R (1989) Pulmonary alveolar proteinosis and cement dust: a case report. J Occup Med 31(3):233–237

Mizuguchi Y, Myojo T, Oyabu T, Hashiba M, Lee BW, Yamamoto M, Todoroki M, Nishi K, Kadoya C, Ogami A, Morimoto Y, Tanaka I, Shimada M, Uchida K, Endoh S, Nakanishi J (2013) Comparison of dose-response relations between 4-week inhalation and intratracheal instillation of NiO nanoparticles using polimorphonuclear neutrophils in bronchoalveolar lavage fluid as a biomarker of pulmonary inflammation. Inhal Toxicol 25(1):29–36

Murali A, Barve A, Leppert VJ, Risbud SH, Kennedy IM, Lee HWH (2001) Synthesis and characterization of indium oxide nanoparticles. Nano Lett 1(6):287–289

Omae K, Nakano M, Tanaka A, Hirata M, Hamaguchi T, Chonan T (2011) Indium lung—case reports and epidemiology. Int Arch Occup Environ Health 84(5):471–477

Rushton EK, Jiang J, Leonard SS, Eberly S, Castranova V, Biswas P, Elder A, Han X, Gelein R, Finkelstein J, Oberdorster G (2010) Concept of assessing nanoparticle hazards considering nanoparticle dosemetric and chemical/biological response metrics. J Toxicol Environ Health A 73(5):445–461

Samedov K, Aksu Y, Driess M (2012) Heterotermetallic indium lithium halostannates: low-temperature single-source precursors for tin-rich indium tin oxides and their application for thin-film transistors. Chemistry 18(25):7766–7779

Sarlo K, Blackburn KL, Clark ED, Grothaus J, Chaney J, Neu S, Flood J, Abbott D, Bohne C, Casey K, Fryer C, Kuhn M (2009) Tissue distribution of 20 nm, 100 nm and 1000 nm fluorescent polystyrene latex nanospheres following acute systemic or acute and repeat airway exposure in the rat. Toxicology 263(2–3):117–126

Sauni R, Jarvenpaa R, Iivonen E, Nevalainen S, Uitti J (2007) Pulmonary alveolar proteinosis induced by silica dust? Occup Med (Lond) 57(3):221–224

Seo WS, Jo HH, Lee K, Park JT (2003) Preparation and optical properties of highly crystalline, colloidal, and size-controlled indium oxide nanoparticles. Adv Mater 15(10):795–797

Stopford W, Turner J, Cappellini D, Brock T (2003) Bioaccessibility testing of cobalt compounds. J Environ Monit 5(4):675–680

Sung JH, Ji JH, Park JD, Yoon JU, Kim DS, Jeon KS, Song MY, Jeong J, Han BS, Han JH, Chung YH, Chang HK, Lee JH, Cho MH, Kelman BJ, Yu IJ (2009) Subchronic inhalation toxicity of silver nanoparticles. Toxicol Sci 108(2):452–461

Toya T, Takata A, Otaki N, Takaya M, Serita F, Yoshida K, Kohyama N (2010) Pulmonary toxicity induced by intratracheal instillation of coarse and fine particles of cerium dioxide in male rats. Ind Health 48(1):3–11

Uchida K, Beck DC, Yamamoto T, Berclaz PY, Abe S, Staudt MK, Carey BC, Filippi MD, Wert SE, Denson LA, Puchalski JT, Hauck DM, Trapnell BC (2007) GM-CSF autoantibodies and neutrophil dysfunction in pulmonary alveolar proteinosis. N Engl J Med 356(6):567–579

Vahter M, Akesson A, Liden C, Ceccatelli S, Berglund M (2007) Gender differences in the disposition and toxicity of metals. Environ Res 104(1):85–95

Wagner GR (1997) Asbestosis and silicosis. Lancet 349(9061): 1311–1315

Warheit DB, Webb TR, Sayes CM, Colvin VL, Re KL (2006) Pulmonary instillation studies with nanoscale TiO2 rods and dots in rats: toxicity is not dependent upon particle size and surface area. Toxicol Sci 91(1):227–236

Zhang H, Ji Z, Xia T, Meng H, Low-Kam C, Liu R, Pokhrel S, Lin S, Wang X, Liao YP, Wang M, Li L, Rallo R, Damoiseaux R, Telesca D, Madler L, Cohen Y, Zink JI, Nel AE (2012) Use of metal oxide nanoparticle band gap to develop a predictive paradigm for oxidative stress and acute pulmonary inflammation. ACS Nano 6(5):4349–4368

Zou X, Liu X, Wang C, Jiang Y, Wang Y, Xiao X, Ho JC, Li J, Jiang C, Xiong Q, Liao L (2013) Controllable electrical properties of metal-doped In2O3 nanowires for high-performance enhancement-mode transistors. ACS Nano 7(1):804–810